AnkB, a Periplasmic Ankyrin-Like Protein in *Pseudomonas aeruginosa*, Is Required for Optimal Catalase B (KatB) Activity and Resistance to Hydrogen Peroxide

MICHAEL L. HOWELL,[1] EYAD ALSABBAGH,[1] JU-FANG MA,[1] URS A. OCHSNER,[2]
MARTIN G. KLOTZ,[3] TERRY J. BEVERIDGE,[4] KENNETH M. BLUMENTHAL,[1]
ERIC C. NIEDERHOFFER,[5] RANDALL E. MORRIS,[6] DAVID NEEDHAM,[7]
GARY E. DEAN,[1] MAQSOOD A. WANI,[1] AND DANIEL J. HASSETT[1]*

*Department of Molecular Genetics, Biochemistry and Microbiology, University of Cincinnati College of Medicine,
Cincinnati, Ohio 45267-0524[1]; Department of Microbiology, University of Colorado Health Sciences Center, Denver,
Colorado 80262[2]; Department of Biology and Center for Genetics and Molecular Medicine, University of Louisville,
Louisville, Kentucky 40292[3]; Department of Microbiology, College of Biological Sciences, University of Guelph,
Guelph, Ontario, Canada N1G 2W1[4]; Department of Medical Biochemistry, Southern Illinois University College of
Medicine, Carbondale, Illinois 62901-4413[5]; Department of Cell Biology, University of Cincinnati College of Medicine,
Cincinnati, Ohio 45267-0521[6]; and Department of Materials Science and Mechanical Engineering, Duke University,
Durham, North Carolina 27708[7]*

In this study, we have cloned the *ankB* gene, encoding an ankyrin-like protein in *Pseudomonas aeruginosa*. The *ankB* gene is composed of 549 bp encoding a protein of 183 amino acids that possesses four 33-amino-acid ankyrin repeats that are a hallmark of erythrocyte and brain ankyrins. The location of *ankB* is 57 bp downstream of *katB*, encoding a hydrogen peroxide-inducible catalase, KatB. Monomeric AnkB is a 19.4-kDa protein with a pI of 5.5 that possesses 22 primarily hydrophobic amino acids at residues 3 to 25, predicting an inner-membrane-spanning motif with the N terminus in the cytoplasm and the C terminus in the periplasm. Such an orientation in the cytoplasmic membrane and, ultimately, periplasmic space was confirmed using AnkB-BlaM and AnkB-PhoA protein fusions. Circular dichroism analysis of recombinant AnkB minus its signal peptide revealed a secondary structure that is ~65% α-helical. RNase protection and KatB- and AnkB-LacZ translational fusion analyses indicated that *katB* and *ankB* are part of a small operon whose transcription is induced dramatically by H_2O_2, and controlled by the global transactivator OxyR. Interestingly, unlike the spherical nature of ankyrin-deficient erythrocytes, the cellular morphology of an *ankB* mutant was identical to that of wild-type bacteria, yet the mutant produced more membrane vesicles. The mutant also exhibited a fourfold reduction in KatB activity and increased sensitivity to H_2O_2, phenotypes that could be complemented in *trans* by a plasmid constitutively expressing *ankB*. Our results suggest that AnkB may form an antioxidant scaffolding with KatB in the periplasm at the cytoplasmic membrane, thus providing a protective lattice work for optimal H_2O_2 detoxification.

Ankyrins are structural proteins in human erythrocytes and brain that bridge the spectrin exoskeleton to the cytoplasmic surface of the plasma membrane (5). They are composed of three domains: (i) an N-terminal membrane-binding domain, (ii) a spectrin-binding domain, and (iii) a C-terminal domain with an apparent regulatory function (5). Integral membrane proteins that associate with ankyrin both in vivo and in vitro include the band III anion exchanger (15), Na^+/K^+-ATPase (15), and multiple sodium channels (51, 52). The protein-binding N-terminal domain harbors a series of 33-amino-acid tandem repeats (herein termed ank repeats) that extend over 740 residues. The tandem repeat motif is present in 22 contiguous copies with 30 to 35% identity between the repeats (reference 5 and references therein). Closely related repeats (30 to 35% identity to brain ankyrin) were found in seemingly dissimilar proteins of lower and higher eukaryotes that regulate the cell cycle in yeast (e.g., products of *cdc10* and *SWI6*) and are involved in intercellular signaling during development and cell differentiation of *Caenorhabditis elegans* (products of *lin-12*, *glp-1*, and *fem-1*), *Drosophila* (Notch), or *Xenopus* (Xotch) (references 2, 9, 19, and 50 and references therein). Subsequently identified ankyrin-like proteins (ALPs) include transcription factors (e.g., GABP-β and NF-κB), toxins (e.g., black widow spider venom), enzymes (e.g., rat liver-specific glutaminase), and a viral host range factor (*Vaccinia hr* gene product) (listed in references 5 and 50); a protein-tyrosine kinase in *Hydra vulgaris* (14); and the *Chlorella* virus long terminal repeat gene product (GenBank accession no. D14469). Two ALPs were also identified in the higher plant *Arabidopsis thaliana* (GenBank accession no. M82883), one of which was implicated in membrane transport (GenBank accession no. X62907). So far, more than 150 genes possessing ank repeats have been reported in eukaryotic systems (GenBank search, May 2000). Due to the success in whole genome sequencing, however, genes encoding ankyrin homologs found most recently reside in bacteria.

The first bacterial ALP-encoding gene (*phlB*), from *Serratia liquefaciens*, was not recognized as such (21) until Bennett (5) identified an ank repeat consensus sequence (-G-TA/PLM/H-AA--GH---V/A--LL--GAD-N/D--D-). According to various

* Corresponding author. Mailing address: Department of Molecular Genetics, Biochemistry and Microbiology, University of Cincinnati College of Medicine, 231 Bethesda Ave., Cincinnati, OH 45267-0524. Phone: (513) 558-1154. Fax: (513) 558-8474. E-mail: Daniel.Hassett @UC.Edu.

databases, bacterial ALPs have been identified in several actinobacteria (*Streptomyces verticillus* [13], *Streptomyces argillaceus* [U43537], *Streptomyces coelicolor* cosmid 6D7 [AL133213]), two spirochetes (*Treponema pallidum* [AE001254] and *Deinococcus radiodurans* [AE002034 and AE001863]), two cyanobacteria (*Anabaena* sp. strain PCC 7120 [X95645] and *Synechocystis* sp. strain PCC 6803 [D90900]), and several proteobacteria (*S. liquefaciens* [21], *Chromatium vinosum* [17], *Rhizobium leguminosarum* [AJ243305], *Rickettsia prowazekii* [AJ235273], *Vibrio cholerae* [http://www.tigr.org], two *Erlichia* species [AF047897 and AF153716], and the four species of fluorescent pseudomonads, i.e., *Pseudomonas aeruginosa* [U59457], *Pseudomonas fluorescens* [U83328], *Pseudomonas putida* KT2440 [http://www.tigr.org], and *Pseudomonas syringae* [32] [AF133262 and AF133263]). Interestingly, unlike eukaryotic ankyrin or ALPs, bacterial ALPs seem to belong to divergent operons: bleomycin and mithramycin antibiotic resistance in *S. verticillus* (13) and *S. argillaceus* (U43537), respectively; periplasmic flavocytochrome *c* and cytoplasmic tetraheme cytochrome *c* in *C. vinosum* (17); and a catalase with proposed periplasmic and cytoplasmic locations in *P. syringae* (32) and *P. fluorescens* (U83328). The ankyrin gene in *V. cholerae* (http://www.tigr.org) is also downstream of a gene encoding a type I bacterial catalase. A putative open reading frame (ORF) upstream of a gene encoding a histidinol phosphate aminotransferase, an enzyme required for ethanol tolerance, was found in *Acetobacter pasteurianus* (DDBJ accession no. D14440) (54). The ALP of *S. liquefaciens*, whose gene is located downstream of the gene encoding periplasmic phospholipase A1, has a putative regulatory function regarding phospholipase activity (21). Taken together, the bacterial ALP genes are located in close proximity to genes encoding proteins involved in either (i) nutrient acquisition and uptake or (ii) tolerance or resistance to antibiotics, starvation, or oxidative stress.

In this study, we demonstrate the first functional characterization of a bacterial ALP, AnkB, in *P. aeruginosa*. AnkB was found to be a cytoplasmic membrane-periplasmic protein whose expression is increased upon exposure of bacteria to H_2O_2. AnkB was also found to be essential for optimal resistance to H_2O_2, which we believe is in part due to its ability to bind to and stabilize KatB, a type I bacterial catalase.

MATERIALS AND METHODS

Bacterial strains, plasmids, and media. All *P. aeruginosa* and *Escherichia coli* strains used in this study are listed in Table 1 and were maintained on Luria (L) agar (10 g of tryptone, 5 g of yeast extract, and 10 g of NaCl) or M9 minimal medium (6 g of Na_2HPO_4, 3 g of KH_2PO_4, 1 g of NH_4Cl, 0.5 g of NaCl, 1 mM $MgSO_4 \cdot 7H_2O$, and 0.2% glucose [per liter]) plates, with each medium solidified with 15 g of Bacto agar per liter. All strains were stored indefinitely at $-80°C$ in a 1:1 suspension of overnight-grown culture and either 25% glycerol or 10% skim milk.

Growth conditions. All bacteria were grown from single-colony isolates or overnight cultures in L broth or M9 minimal medium. Liquid cultures were grown at 37°C with shaking at 300 rpm or on a roller wheel at 70 rpm unless otherwise indicated. Culture volumes were 1/10 of the total Erlenmeyer flask volume to ensure proper aeration.

Cloning and sequence analysis of *ankB*. Steps involved in the cloning of the *P. aeruginosa* PAO1 *ankB* and *radA* genes are described in Results. DNA sequencing was performed on both strands using the PRISM Dye Deoxy Terminator Cycle Sequencing Kit and analyzed on an ABI model 373A DNA sequencer. Oligonucleotides for DNA sequencing reactions and PCR analysis were synthesized in the DNA Core Facilities in the Department of Molecular Genetics, Biochemistry and Microbiology at the University of Cincinnati College of Medicine or in the Department of Microbiology at the University of Colorado Health Sciences Center. Sequence analyses were performed using either MacVector 6.5.1 (Eastman Chemical Co., New Haven, Conn.), Sequencher 3.1 (Gene Codes Corp., Ann Arbor, Mich.), or Gene Runner (Hastings Software, Inc.) software. Amino acid alignments were performed using either the BLASTP program provided by the National Center for Biotechnology Information (1) or the Align Plus 3 Global Alignment Program (Sci-Ed Software, Durham, N.C.). Potential

membrane-spanning domains (MSDs) of AnkB and other bacterial ankyrin-like proteins were determined using TOP-PRED II (57) or the SOSUI program (http://www.tuat.ac.jp/~mitaku/adv_sosui/submit.html).

Manipulation of recombinant DNA and RNA. Plasmid DNA was transformed into *E. coli* DH5α-MCR (Gibco-BRL, Gaithersburg, Md.) or SM10 (48). 5-Bromo-4-chloro-3-indolyl-β-D-galactopyranoside (X-Gal) (40 μg/ml) was routinely added to agar medium to detect the presence of insert DNA. Restriction endonuclease, alkaline phosphatase (AP), Klenow fragment, T4 DNA polymerase, and T4 DNA ligase were used as specified by the vendor (Gibco-BRL). Plasmid DNA was isolated using miniprep kits from Qiagen. DNA fragments used for cloning or in the construction of radiolabeled probes were recovered from agarose gels using SeaPlaque low-melting-point agarose (FMC BioProducts, Rockland, Maine) or with the GeneClean II kit (BIO 101, Inc., La Jolla, Calif.). RNA was isolated by the hot-phenol method and analyzed by RNase protection assays as described in detail elsewhere (3). Radiolabeled riboprobes were generated from cloned DNA fragments (Table 1) using an in vitro runoff transcription system (Promega), and excess probe was hybridized to 20 μg of total RNA.

Overexpression of recombinant AnkB in *E. coli*. Overexpression of recombinant AnkB as a His6-tagged protein in *E. coli* was performed using the T7 promoter-T7 RNA polymerase system (53). A 0.53-kb fragment containing the *ankB* gene minus the first 19 codons comprising its signal sequence was amplified using primers (*Xho*I)-ctCGAGGTGCATGGGGTCGAGGT and (*Bam*HI)-gga TCCAGACTAGCCCAGCAGGC (bases in the *Xho*I and *Bam*HI restriction sites are underlined, and nonmatching bases near the 5′ end are in lowercase type). This PCR product was cloned into pCRII (Invitrogen), sequenced, and directionally cloned as an *Xho*I-*Bam*HI fragment into pET14b (Novagen). The resulting plasmid, pET14b-*ankB*, allowed T7-inducible expression of AnkB containing an in-frame His6 tag at its N terminus spaced by a thrombin cleavage site encoded on pET14b. Similarly, a 0.485-kb fragment containing the *ankB* gene minus the first 17 codons and lacking the last two codons was amplified using the primers (*Nhe*I)-GCTaGCGAGGTGCATGGGGTCGA and (*Not*I)-GCgGCCG CAGTGCCGTTCAGTTC and subsequently cloned as an *Nhe*I-*Not*I fragment into pET23a linearized with *Nhe*I and *Not*I. In the resulting plasmid, pET23-*ankB*, the AnkB protein was fused in frame to a carboxy-terminal His6 tag encoded by pET23a. Recombinant plasmids were first selected in *E. coli* DH5α-MCR and then transformed into *E. coli* BL21(λDE3), which harbors a single genomic copy of the T7 RNA polymerase gene under control of the *lacUV5* promoter. These bacteria were grown in 1 liter of L broth containing ampicillin at 100 mg/ml to an optical density at 600 nm (OD_{600}) of 0.3. At this point, the synthesis of T7 polymerase was induced by the addition of 0.5 mM isopropyl-β-D-thiogalactopyranoside (IPTG), and the cells were allowed to grow for an additional 3 h at 37°C. Recombinant AnkB proteins were then purified using a nickel-nitrilotriacetic acid column as specified by the manufacturer (Qiagen).

Construction of *ankB::blaM*, *ankB::phoA*, and *ankB::lacZ* fusion plasmids. For construction of a translational *ankB::blaM* fusion plasmid, the N-terminal region of *ankB* was PCR amplified to create a 551-bp fragment harboring the entire *ankB* gene. This fragment was cut with *Nae*I, and the 162-bp 5′ fragment containing the predicted MSD and a portion of the predicted periplasmic region of AnkB was ligated into the *Sma*I site of pKM1 (10). For construction of a translational *ankB::phoA* fusion plasmid, a 174-bp 5′ fragment of the *ankB* gene containing an *Afl*III restriction site was first cloned into a T/A version of pKS(−) (35). The *ankB* fragment was removed from this plasmid and cloned into the *Nco*I-*Sma*I sites of pEX30 (H. P. Schweizer). pPHO7, a broad-host-range *phoA*-containing plasmid encoding AP (24), was first cut with *Bam*HI, blunted, and then excised with *Pst*I. The resulting *phoA* gene was then ligated to pEX-*ankB* that had been previously digested with *Eco*RI (blunted) and *Pst*I, allowing for directional cloning of *ankB* in frame with *phoA*. The resulting construct fuses the first 58 amino acids of AnkB with PhoA. Translational fusions of *ankB* to the *lacZ* reporter gene were constructed as follows. PCR products were generated with primer (*Bam*HI)-ggatCCTCGCATCGTCGTCATCTC containing a *Bam*HI site after the third codon of the *ankB* gene and either primer TACAA GGCTGACAGCGACT (0.16 kb upstream), primer GCAGCGAGGTCAATA CCGTC (0.47 kb upstream), or primer CTTGGAACTGCGCCATGCAG (1.9 kb upstream). The PCR products were cloned into pCRII and directionally ligated as *Eco*RI-*Bam*HI fragments into pPZ30 linearized with *Eco*RI and *Bam*HI, yielding pPZ-*ankB*-160, pPZ-*ankB*-470, and pPZ-*ankB*-1900, respectively.

Construction of isogenic *P. aeruginosa* *ankB* and *katB* *ankB* mutants. To generate a clean Δ*ankB* deletion mutant, the DNA sequences flanking *ankB* were PCR amplified using primers GCAGCGAGGTCAATACCGTC and (*Kpn*I)-ggtaCCGGTTGCGATCAATCCTGG (0.408-kb *ankB* upstream fragment) and primers (*Xba*I)-tctaGATGCGTTGGGCAACAGCGT and (*Hin*dIII)-aaGCTTCAACCCCTGCAGCGCCA (0.334-kb *ankB* downstream fragment). The two PCR products were cloned into pCRII, sequenced, and cloned as an *Eco*RI-*Kpn*I *ankB* upstream fragment and an *Xba*I-*Hin*dIII *ankB* downstream fragment on each side of and in proper orientation to a 1.7-kb *aac1* (Gm^r) cartridge in pUC-Gm, yielding pUCΔ*ankB*::Gm. A 2.8-kb *Pvu*II fragment of pUCΔ*ankB*::Gm containing the Δ*ankB*::Gm construct was cloned into the *Sma*I site of the suicide vector pEX100T (46), and the resulting pEX100T-Δ*ankB*::Gm was transformed into *E. coli* SM10, which then served as the donor strain in a biparental plate mating (16 h, 37°C) with *P. aeruginosa* PAO1 or with PAO1 Δ*katA*::Tc (35). The mating mixture was plated on brain heart infusion agar

TABLE 1. Strains and plasmids used in this study

Strain or plasmid	Genotype or characteristics[a]	Source or reference
E. coli strains		
HB101	*proA2 leuB6 thi-1 lacY1 hsdR hsdM recA13 supE44 rpsL20*	H. Boyer
DH5α	F⁻ *lacZ*ΔM15 *recA1 hsdR17 supE44* Δ(*lacZYA argF*)	Bethesda Research Laboratories
SM10	Km^r; mobilizer strain	48
BL21(DE3)	F⁻ *dcm ompT hsdS gal* λ (DE3); T7 polymerase gene under control of the *lacUV5* promoter	53
P. aeruginosa strains		
PAO1	Prototrophic, wound isolate	28
PAO1 Δ*ankB*::Gm	Gm^r; deletion of 0.526 kb of the *ankB* gene	This study
PAO1 *katA*::Tc	Gm^r; *katA*::Tc mutant	35
PAO1 Δ*katA* Δ*ankB*	Gm^r Tc^r; deletion of 0.526 kb of the *ankB* gene in a PAO1 Δ*katA* background	This study
PAO1 *katB*::Gm	Gm^r; *katB*::Gm mutant	18
PAO1 Δ*katB ankB*::Gm	Gm^r; deletion of 1.75 kb of the *katB-ankB* locus	This study
PAO1 *radA*	Gm^r; *radA*::Gm mutant	This study
Plasmids		
pBluescript KS(−/+)	Ap^r; extended polylinker pUC derivative	Stratagene
pKS-T/A	Ap^r; T/A vector using the *Eco*RV site for cloning	35
pKS-*ankB*	Ap^r; 174-bp 5′ fragment of *ankB* in *Eco*RV site	This study
pUCP22	Ap^r; broad-host-range extended polylinker pUC derivative	44
pUCP22-*ankB*	pUCP22 containing a 0.825-kb *Eco*RI-*Hin*dIII fragment with the *ankB* gene under *lac* promoter control	This study
pET14b	Expression vector; Ap^r	Novagen
pET14b-*ankB*	pET14b containing *ankB* with an amino-terminal His$_6$ tag under T7 promoter control	This study
pET23a	Expression vector; Ap^r	Novagen
pET23a-*ankB*	pET23a containing *ankB* with a carboxy-terminal His$_6$ tag under T7 promoter control	This study
pEX30	Ap^r; broad-host-range expression vector	H. P. Schweizer
pEX30-*ankB*	Ap^r; pEX30 with a 193-bp *Afl*III-*Sma*I *ankB* fragment within the *Nco*I-*Sma*I sites	This study
pEX30-*ankB*::*phoA*	Ap^r; pEX30-*ankB* with a 2.6-kb *phoA*-containing fragment of pPHO7 fused to *ankB*	This study
pEX100T	Ap^r; *oriT mob sacB* gene replacement vector	46
pEX100T-Δ*ankB*::Gm	pEX100T carrying a 2.8-kb Δ*ankB*::Gm gene study replacement construct	This study
pEX100T-Δ*katB ankB*::Gm	pEX100T carrying a 2.6-kb Δ*katB ankB*::Gm gene study replacement construct	This study
pKM1	Ap^r; broad-host-range *blaM* β-lactamase fusion plasmid	10
pPHO7	Ap^r; broad-host-range *phoA* alkaline phosphatase fusion plasmid	24
pPZ30	Ap^r; broad-host-range *lacZ*-based promoter probe vector	43
pPZ-*ankB*-1900	pPZ30 containing a 1.9-kb fragment of the *katB-ankB* region including the *katB* promoter	This study
pPZ-*ankB*-470	pPZ30 containing a 0.47-kb fragment of the *ankB* upstream region	This study
pPZ-*ankB*-160	pPZ30 containing a 0.16-kb fragment of the *ankB* upstream region	This study
pUCGM	Gm^r; pUC19 plus 850-bp *aaC1* cassette	45

[a] Abbreviations used for genetic markers were as described by Holloway et al. (29). *mob*, mobilization site (ColE1); Tra⁺, conjugative phenotype; *oriT*, origin of transfer (RK2); Ap^r, ampicillin resistance; Cm^r, chloramphenicol resistance; Gm^r, gentamicin resistance; Km^r, kanamycin resistance.

containing gentamicin (75 μg ml⁻¹) and irgasan (Ciba-Geigy) (50 μg ml⁻¹) as a counterselective agent. Several colonies were grown to late logarithmic phase in L broth, and serial dilutions were spread onto L agar containing gentamicin (75 μg ml⁻¹) and sucrose (5%). Chromosomal DNA from individual colonies was evaluated for deletion of the *ankB* gene by PCR and Southern blot analysis (data not shown). A PAO1 Δ*katB ankB* deletion mutant was obtained as follows. A 2.7-kb fragment containing the *katB-ankB* region was PCR amplified using the primers CTTGGAACTGCGCCATGCAG and GCTTCAACCCCTGCAGCG CCA and cloned into pCRII. A 1.75-kb *Sst*II fragment containing most of the *katB* and *ankB* genes was excised and replaced by a 1.2-kb Gm^r cartridge by blunt-end ligation after filling in the ends with Klenow enzyme. A 2.6-kb *Pvu*II fragment of the resulting plasmid, pCRII-Δ*katB ankB*::Gm, was cloned into the *Sma*I site of pEX100, yielding the donor plasmid pEX100T-Δ*katB ankB*::Gm for a mating as described above.

Cell fractionation: periplasm, cytoplasm, and cytoplasmic membrane. Bacteria were grown aerobically in 1 liter of L broth at 37°C until the OD$_{600}$ reached 0.6. At this point, organisms were treated with 350 μM paraquat (Sigma) for 1 h to stimulate *katB-ankB* transcription prior to harvesting the bacteria by centrif-

ugation at 10,000 × *g* for 10 min. The pellet was washed twice in ice-cold 10 mM Tris-HCl–30 mM MgCl$_2$ (pH 7.3) (Tris-Mg) and resuspended in 1/25 the volume of the same buffer. Chloroform (15 μl/ml of buffer) was then added, and the cells were incubated on ice for an additional 15 min followed by dilution with an additional 1 ml of buffer. The bacteria were pelleted by centrifugation at 10,000 × *g* for 10 min at 4°C, and the supernatant was further subjected to centrifugation at 150,000 × *g* for 2 h at 4°C to remove potential contaminating membranes. Finally, the periplasmic preparation was stored on ice. The bacteria were washed again, resuspended in 5 ml of Tris-Mg, and disrupted by sonication with a Heat Systems-Ultrasonics (Farmingdale, N.Y.) model W-225 sonicator equipped with microtip at output setting 5 at 4°C. Cell debris and membrane fractions were clarified by centrifugation at 35,000 × *g* for 1 h at 4°C. The supernatant was designated the cytoplasmic fraction.

For preparation of cytoplasmic membrane proteins, the above-described growth conditions were employed. The pellet of paraquat-stimulated bacteria was resuspended in 10 ml of 10 mM Tris-HCl (pH 7.5) (T buffer), containing 20% sucrose, treated with 0.5 mg of DNase I (Gibco) and RNase (Sigma) per ml, and incubated for 15 min at 22°C with periodic agitation. The suspension was
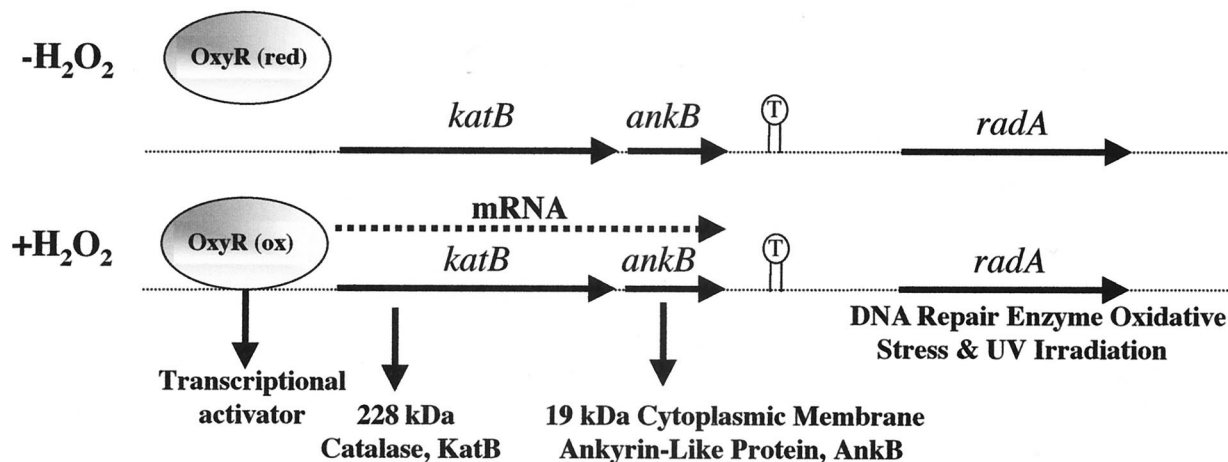
FIG. 1. Gene map of the ~5.2-kb insert of pSMB1 containing the *katB*, *ankB*, and *radA* genes. The functions of the gene products are also given. We have previously shown that OxyR, a 34-kDa transactivator, responds to H_2O_2 by activating *katB-ankB* (39). T, 33-amino-acid inverted repeat that could represent the transcriptional terminator for the *katB-ankB* operon.

placed on ice for 20 min, followed by two passages through a French pressure cell at 1,200 lb/in² at 4°C. The cell debris was removed by centrifugation at 5,500 × *g* for 10 min at 4°C. The supernatant containing the membranes was subjected to a two-stage sucrose gradient centrifugation. The first stage involved layering 10 ml of membranes on 14 ml of 50% sucrose and 14 ml of 70% sucrose in T buffer. The membranes were then separated by centrifugation in an SW28 swinging-bucket rotor at 130,000 × *g* for 17 h at 4°C. Cytoplasmic membranes (the top red band) and outer membranes (the bottom white band) were collected by dropwise collection and diluted to 7 ml in cold T buffer–20% sucrose. The second centrifugation stage involved layering the membrane fractions on 9 ml of 52% sucrose, 9 ml of 58% sucrose, 9 ml of 64% sucrose, and 3 ml of 70% sucrose, each prepared in T buffer. The membranes were again separated by centrifugation in an SW28 swinging bucket rotor at 130,000 × *g* for 17 h at 4°C. The purified cytoplasmic and outer membrane fractions were concentrated by dropwise collection and dialyzed exhaustively against T buffer for 17 h at 4°C. The purity of each cellular fraction was gauged by measuring enzymatic activities specific for the cytoplasm, periplasm, and inner membrane. Stripping of AP activity from cytoplasmic membrane preparations was accomplished by incubating the membranes in either T buffer (control) or 0.1 M Na₂CO₃ for 30 min on ice. Thirty milliliters of the membrane suspension was carefully layered on 4 ml of 0.3 M sucrose in T buffer and centrifuged at 150,000 × *g* for 2 h at 4°C. The pellet was solubilized in 2% Triton X-100 in T buffer and assayed for AP activity as described below. Glucose-6-phosphate dehydrogenase, a cytoplasmic marker, was assayed by monitoring the reduction of NADP⁺ at 340 nm as previously described (33). β-Lactamase, one periplasmic marker, was assayed by the decomposition of 50 μM nitrocefin (CalBiochem, La Jolla, Calif.) at 486 nm (34). AP, another periplasmic marker, was assayed by monitoring the production of *p*-nitrophenol through hydrolysis of 1 mM *p*-nitrophenyl phosphate (Sigma) (20). AP activity in bacterial colonies on L-agar plates containing 10 mM potassium phosphate (pH 7.0) to inhibit endogenous AP activity was monitored using 5-bromo-4-chloro-3-indolyl phosphate (BCIP) (40 μg/ml) in the medium. Succinate dehydrogenase, a cytoplasmic membrane marker, was assayed by monitoring the reduction of dichlorophenol-indophenol as previously described (12).

TEM. Cells were harvested from exponential-growth-phase cultures, treated with 1 mM H_2O_2 to induce the *katB-ankB* operon, and negatively stained for transmission electron microscopy (TEM). For staining, the cells were put on a carbon- and Formvar-coated 200-mesh TEM grid, stained for 15 s with 2% (wt/vol) uranyl acetate, and blotted dry. The negatively stained bacteria were imaged using a Philips EM300 instrument operating at 60 kV under standard conditions with the liquid nitrogen anticontaminator in place.

Circular dichroism spectropolarimetry. Circular dichroism spectra of purified recombinant AnkB proteins (AnkB-23a and AnkB-14b) were obtained using a JASCO J-710 spectropolarimeter calibrated with d_{10}-camphorsulfonic acid. All samples were dissolved in 10 mM sodium phosphate (pH 7.0) and equilibrated at 22°C for 10 min prior to data collection. The spectra represent the means of four independent scans obtained at a scanning rate of 20 nm min⁻¹. Samples were added to a water-jacketed, cylindrical quartz cuvette with a 0.05-cm path length. Protein content was calculated based upon the equation [protein]$_{\mu g/ml}$ = $144(A_{215} - A_{225})$, using a 1-cm light path. Percent α-helix was estimated from $[\theta]_{222}$ as described by Greenfield and Fasman (23).

Cell extract preparation and biochemical assays. Routine cell extracts were prepared from bacteria harvested by centrifugation at 10,000 × *g* for 10 min at 4°C. Bacteria were washed twice in ice-cold 50 mM potassium phosphate buffer

(pH 7.0) and sonicated in an ice-water bath for 10 s as described above. The sonicate was then clarified by centrifugation at 13,000 × *g* for 10 min at 4°C. Cell extract preparation for native gel electrophoresis was performed as described above except that 50 mM T buffer was used as the diluent. Catalase activity was assayed spectrophotometrically at 240 nm by monitoring the decomposition of 18 mM H_2O_2 using a Spectronic Genesys 5 spectrophotometer (Spectronic Unicam, Rochester, N.Y.) (4). The concentration of H_2O_2 was determined using an extinction coefficient of 43.6 mM. One unit of activity is that which degrades 1 μmol of H_2O_2 per min at 23°C. Nondenaturing polyacrylamide gels (5%) were stained for catalase activity according to the method of Wayne and Diaz (58). β-Galactosidase assays were performed using *o*-nitrophenyl-β-D-galactopyranoside, and the results were expressed as international units with an extinction coefficient for *o*-nitrophenyl-β-D-galactopyranoside of 3.1 mM (37). Protein concentrations in cell extracts were estimated by the method of Bradford (8), using bovine serum albumin as a standard.

Nucleotide sequence accession number. The *P. aeruginosa katB*, *ankB*, and *radA* sequences have been assigned GenBank accession number U89384.

RESULTS

Sequence analysis downstream of the *P. aeruginosa katB* gene: identification of *ankB*, encoding an ALP, and *radA*, a DNA repair protein. In a previous study, we cloned and characterized the *katB* gene, encoding a 228-kDa tetrameric catalase (11). The *katB* gene was recently found to be under the control of the global transactivator OxyR (39), and its transcription is markedly induced upon exposure to H_2O_2 or the redox-cycling agent paraquat (11). DNA sequence analysis downstream of the *katB* locus revealed a small, 549-bp ORF (Fig. 1). This ORF, *ankB*, is predicted to encode a protein of 183 amino acids with a monomeric molecular mass of 19,360 Da and a pI of 5.55. The deduced amino acid sequence demonstrated the highest similarity with genes harboring ank repeats in other bacteria (13, 17, 21, 32) and various ankyrin or ALP genes in eukaryotes (5) (see below). When we sequenced further downstream of the *ankB* locus, we discovered a large inverted repeat spanning 33 bp (Fig. 1). We then identified a gene downstream of the inverted repeat that was 70% identical to the *radA* gene of *E. coli* (49). The *radA* gene in *E. coli* encodes a protein that repairs DNA damaged (alkylated) by gamma irradiation. However, because virtually nothing is known about the function of ALPs in bacteria, we chose to focus our efforts on the functional characterization of *P. aeruginosa* AnkB.

Amino acid comparison of AnkB with other bacterial ALPs. Ankyrins are proteins that are characterized by 33-amino-acid

```
CvAnkA                 MDPIRTSRLRAPLLASALLLAGSSV     CAAEPDLETELRLNAMIGDTETAAELLDQGAHV
RBC                                                  N--D--G-TPLH-AA--GH---V--LL--GAD-
                                                        N      A M V


PaAnkB                                                                              MRG
PsAnkF                                                                              MK-
CvAnkA                 DAPNQFGKTALMFAVEGDDLETVALLLSRGADV     NARTVAGCTPLTFAAEAGHIGISALLLERGAHV
SlPhlB                                             MPEG     RRLRRALAIALLALVAVTGLLMMAKEQQMGNEI
RBC                    N--D--G-TPLH-AA--GH---V--LL--GAD-     N--D--G-TPLH-AA--GH---V--LL--GAD-
                          N      A M V                         N      A M V


PaAnkB     WILAGWLLAALAAQA------------GEVHG     VEVEARLRDYFFDAARRGDQAMLKEFVEAGFDL
PsAnkF     HLIYGLLLFAAAANATPPTSTTTPTPPPPELTA     EQTASQLRTLFFDASREGNNPMLDTFIEAHYDL
CvAnkA     HDRTRSGWDALMIASRHGITDMVEQLLFKGADP     KAADREGRTALMQAASKGETGVLPLLIEGGADL
SlPhlB     SPFDGHSNLALANAVARGDTNGIHANATNDRLR     ERGDRNV-TLLNWAVLSNNPDSVNALLDLGADP
SvAnkA                                          MGDSATAPALVEAARNGDLAALQAAVAAGADL
RBC        N--D--G-TPLH-AA--GH---V--LL--GAD-     N--D--G-TPLH-AA--GH---V--LL--GAD-
              N      A M V                         N      A M V


PaAnkB     DVQDAKGYTALILAAYHGHGGAVEQLLEAGADP     CVQDARGNTALMGAIFKGEVRIARRLIGAQCSP
PsAnkF     NIRDEQGYTGLILAAYHGHEDSVIRLIDAGADP     CAKDNRGNTALMGAIFKGELSIAKRLVQADCGA
CvAnkA     EARDKQGATALLIAADQGQAGAVETLAGLGAQL     DAVDALGSTALILAVGHGHVAMVERLLAMGADP
SlPhlB     AAAGLDGNSALHTAAMLNDANYLRLLLAEGANM     NVRNAVTGATPLAAAVLAGREENLRLLLAAGADT
SvAnkA     TARDDDDWSALDRAAGLGDVAAVRALLAAGADP     GAVGREARPPYEIALAAGHLDAARELRAAE-DA
RBC        N--D--G-TPLH-AA--GH---V--LL--GAD-     N--D--G-TPLH-AA--GH---V--LL--GAD-
              N      A M V                         N      A M V


PaAnkB     DQRNGAGQTAAMYAALFKREELLQALSARGADL     GARDALGNSVESLRRGELNGTAAAR*
PsAnkF     NLTNNAGQTAAMYAALFKRTEVLKELTDKGADL     SIRDSMGNDVEGLSKW*
CvAnkA     NRQDRKGTTALMEAVATDHAELIDRLIAAGART     DLKDDADRTAADIAVQLGHRQAIARLAPKASKT
SlPhlB     TLSDRLGDTPLHLAAKINRRTWRCCCCRPGPMP     GRATSRASRSSFTSRGRRRICRMTN*
SvAnkA     ASGPAAAPRRTWEPYCRAYPVAELARYPRWEER     GESDEEEDGAASTVFYLHHDLTVTRSIWHGEDV
RBC        N--D--G-TPLH-AA--GH---V--LL--GAD-     N--D--G-TPLH-AA--GH---V--LL--GAD-
              N      A M V                         N      A M V


CvAnkA     P*
SvAnkA     VFDAVTPEWDRFCRDELAFAAPDDFDLVP*
```

FIG. 2. Alignment of the deduced amino acids from genes coding for bacterial ankyrins PaAnkB (*P. aeruginosa*; accession no. U59457), PsAnkF (*P. syringae*; U16026), CvAnkA (*C. vinosum*; L13419), SlPhlB (*S. liquefaciens*; P18954), and SvAnkA (*S. verticillus*; L26954). The 33-amino-acid tandem repeats (underlined) were revealed by using the Ank motif of conserved residues (boldface) as identified by Bennett using the erythrocyte ank repeat consensus sequence (5). Proposed signal sequences are indicated by a double underline. The conserved ank repeat sequences for erythrocyte ankyrin are given below the selected bacterial ALP sequences. RBC, erythrocyte concensus ank repeat sequence.

ank repeats that are thought to represent an ancient motif that has evolved to allow for functional diversity without compromising specificity (5). Each of the five bacterial ALPs in Fig. 2 possess the 33-amino-acid tandem, nonidentical ank repeats. These repeats are based upon the consensus ank repeat motif put forth by Michaely and Bennett (36). AnkB (PaAnkB), not surprisingly, is similar to AnkF (PsAnkF, in the related plant pathogenic species *P. syringae*, strain 61 [32]; PsAnkB [in *P. syringae* B301D; accession no. AF133262]; and PfAnkB [in *P. fluorescens*; U83328]) in that it possesses four tandem repeats and an 18-residue signal sequence (Fig. 2). However, the Ank signal peptides from *P. syringae* differ from those of PaAnkB

and PfAnkB in that they are followed by a proteolytic proline-threonine-box (hinge [32]). Interestingly, PaAnkB and PfAnkB, but not PsAnkF and PsAnkB, possess an RGD motif, which, in eukaryotes, is responsible for physical interaction with integrins, structural proteins that play a role in the homing and action of immune cells. Other bacterial ALPs (some of which are not listed in Fig. 2) from *V. cholerae* (http://www.tigr.org/.) (VcAnkB), *S. argillaceus* (U43537) (SaAnk), *C. vinosum* (17) (CvAnkA), and *S. liquefaciens* (21) (SlPhlB, for phospholipase A1-related ALP) possessed longer putative signal sequences (25 to 28 residues), while the ALP from *R. leguminosarum* (AJ243305) (R1Ank) contained a very short
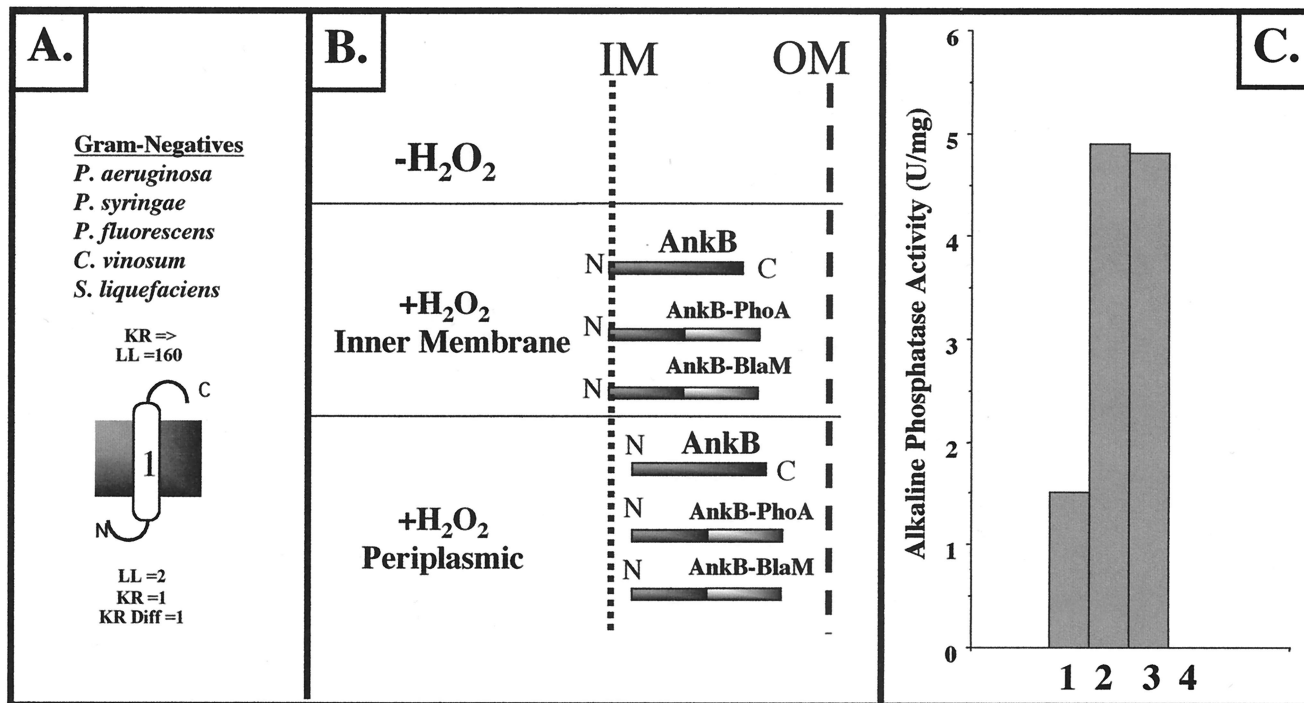
FIG. 3. Cellular localization of AnkB in *P. aeruginosa*. (A) Predicted cytoplasmic membrane organization of *P. aeruginosa* AnkB bacterial ankyrin-like proteins from *P. syringae*, *P. fluorescens*, *S. liquefaciens*, and *C. vinosum* based upon the positive-inside-rule algorithm developed by von Heijne (57). For the *P. aeruginosa* AnkB protein, the large number 1 indicates the predicted single MSD. N, N terminus; C, C terminus; LL, loop length; KR, number of lysine and arginine residues; KR Diff, positive charge difference. (B) Schematic diagram of AnkB–β-lactamase and AnkB-PhoA protein fusions in both *E. coli* and *P. aeruginosa* PAO1. In both cases, organisms expressing AnkB–β-lactamase were resistant to ampicillin (*E. coli*) or carbenicillin (*P. aeruginosa*). Organisms expressing AnkB-PhoA were found to hydrolyze the alkaline phosphatase substrate BCIP in L-agar plates. IM, inner membrane; OM, outer membrane. (C) AP activity in cellular fractions of *P. aeruginosa* *ankB* harboring pEX30-*ankB*::*phoA*. Bar 1, cytoplasm; bar 2, periplasm; bar 3, cytoplasmic membrane; bar 4, outer membrane.

N-terminal MSD of 12 residues. The ALPs of *S. verticillus* (13) (SvAnkA and SvAnkB) possessed only two 33-amino-acid ank repeats. All other identified bacterial ALPs contain a putative cleavage site following an MSD either in the middle or close to the C terminus, or they do not contain a hydrophobic region long enough to incorporate into the membrane.

AnkB is a periplasmic protein: AnkB–β-lactamase and AnkB-alkaline phosphatase protein fusion analysis. Using the membrane topology program TopPred 3.0, it was predicted that the cytoplasmic N terminus of *P. aeruginosa* AnkB (3 amino acids) is followed by a 20-amino-acid stretch that is predicted to be the hydrophobic inner-MSD (for a von Heijne schematic, see Fig. 3A) (TMRGWILAGLL-LAALAAQAEVH), with the remaining portion of the protein (being highly hydrophilic) predicted to reside in the periplasm. The ALPs of other selected gram-negative bacteria, including *C. vinosum*, *S. liquefaciens*, and other *Pseudomonas* species, are also predicted to span the cytoplasmic membrane (Fig. 3A). To test whether the predicted cytoplasmic membrane location was correct, we constructed AnkB-BlaM and AnkB-PhoA protein fusions linking the C terminus of AnkB with both reporters (Fig. 3B). *E. coli* and *P. aeruginosa* harboring an *ankB*::*blaM* fusion plasmid were resistant to ampicillin and carbenicillin, respectively. In addition, *E. coli* and *P. aeruginosa* harboring pEX30-*ankB*::*phoA* were blue on indicator plates containing BCIP, suggesting that the C terminus of AnkB resides in the periplasm and confirming the AnkB–β-lactamase fusion plasmid results. To determine the precise location of AnkB within the cell, membrane fractionation techniques (see Materials and

Methods) were employed. Cytoplasm, periplasm, cytoplasmic membrane, and outer membrane fractions were assayed for AP activity (Fig. 3C). The vast majority of AP activity was detected in the periplasmic space and the cytoplasmic membrane. The contaminating AP activity in the cytoplasm is likely due to overexpression and problems associated with transport of a larger-than-normal AnkB-PhoA protein. To show that AnkB traverses the cytoplasmic membrane and is not simply nonspecifically bound to it, cytoplasmic membranes were stripped by treatment with Na_2CO_3 at high pH (56). Our results showed that AnkB is tightly bound to the cytoplasmic membrane (data not shown). These results suggest that AnkB first exists as a cytoplasmic membrane protein, followed by proteolytic cleavage via a putative LepB signal peptidase cleavage site (GEVHG) to finally reside in the periplasmic space (42).

Overexpression of AnkB in *E. coli*: AnkB secondary structure is predominantly α-helical. To obtain some preliminary structural analysis of AnkB, we overexpressed and purified two recombinant AnkB proteins with N-terminal (pET23a-AnkB) and C-terminal (pET14b) His$_6$-tagged fusions in *E. coli* BL21(λDE3) without their predicted MSDs. Figure 4A demonstrates purified pET23a-AnkB. Gorina and Pavletich revealed that the secondary structure of an ank repeat in protein 53BP2, which binds to the p53 tumor suppressor, consists of an L-shaped structure with a β-turn and 2 α-helices (22). Circular dichroism spectropolarimetric analysis of recombinant AnkB-23a suggested that AnkB is ~60 to 70% α-helical (Fig. 4B). This structure is consistent with the 66% α-helical nature of the ank repeats of the 53BP2 protein (22).
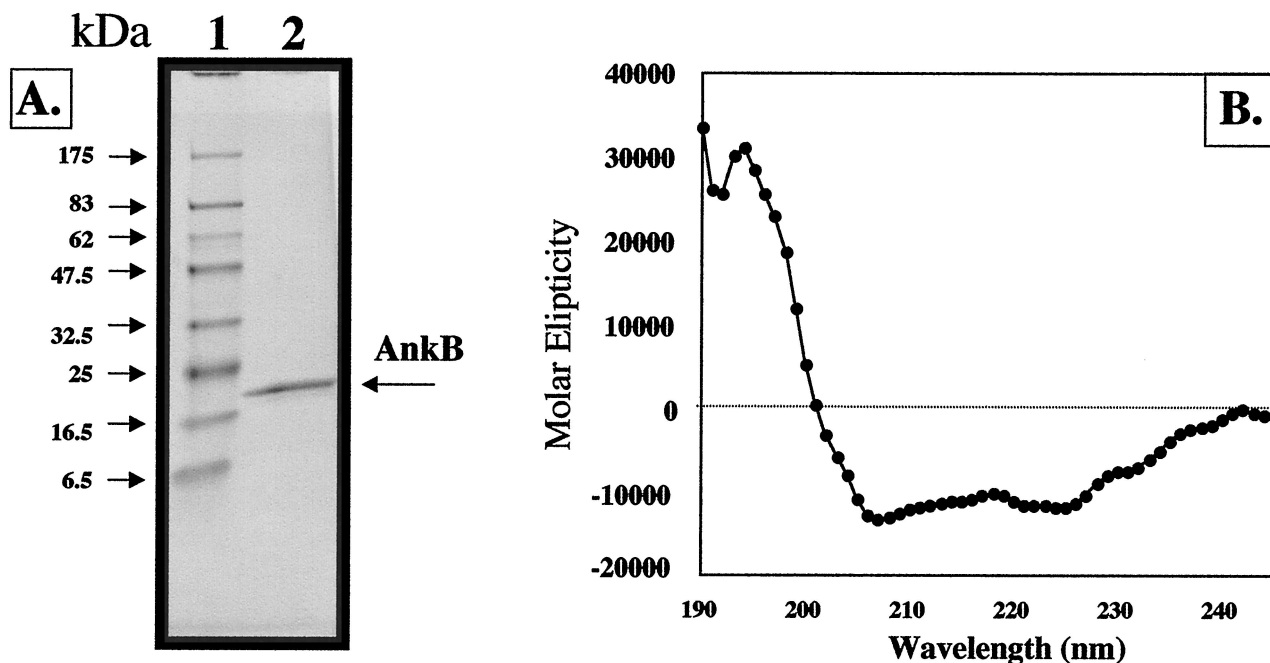
FIG. 4. Overexpression (A) and circular dichroism analysis (B) of recombinant AnkB proteins. (A) *E. coli* BL21(λDE3) harboring pET23-*ankB*-480 was grown aerobically in L broth to mid-logarithmic phase and treated with 1 mM IPTG for 3 h at 37°C. After Ni^{2+}-nitrilotriacetic acid purification, purified protein was separated by sodium dodecyl sulfate–12% polyacrylamide gel electrophoresis and the gel was stained with Coomassie blue R-250. Lane 1, molecular mass standard; lane 2, 15 μg of AnkB-480. (B) Circular dichroism spectrum of AnkB-480, using 100 μg ml^{-1} in 10 mM sodium phosphate (pH 7.0) at 23°C.

Polycistronic nature of *katB* and *ankB*: regulation by H$_2$O$_2$. To determine if *katB* and *ankB* are part of a small operon, RNase protection assays were performed. Figure 5 demonstrates that transcription of both *katB* and *ankB* is stimulated by paraquat in a concentration-dependent fashion. The transcriptional start site was found to be a G 227 bp upstream of the *katB* start codon. Furthermore, transcription of *katB*-*ankB* is dependent upon OxyR, since no *katB* and very little *ankB* transcript could be detected in an *oxyR* mutant. These results were also confirmed using *ankB*::*lacZ* reporter fusion studies (data not shown).

Phenotypes of a *P. aeruginosa ankB* mutant. (i) Normal cell size and shape. Humans with hereditary spherocytosis (HS) suffer from an ankyrin deficiency. Erythrocytes from individuals with HS lack deformability and stability (40) and are unable to pass through capillaries, resulting in hemolytic anemia and hypersensitivity to osmotic lysis. This disorder has been reproduced in nb/nb (normoblastosis, ankyrin-deficient) mice (7), which have a severe hemolytic anemia throughout life (41). In these settings, it is predicted that a loss of ankyrin from the lipid bilayer causes a reduction in the critical surface area/volume ratio, leading to a shift in the morphology of erythrocytes from discoidal to spherical. Thus, there is a definitive structural role for ankyrins in erythrocytes. In contrast to the case for HS erythrocytes, the ultrastructure of wild-type and *ankB* mutant bacteria was observed by TEM and no significant differences in overall cell shape were found (Fig. 6). However, the *ankB* mutant produced more membrane vesicles than wild-type bacteria (Fig. 6B). This implies that a fundamental difference exists between the surfaces of the wild type and the *ankB* mutant and that their ability to package periplasmic constituents in natural membrane vesicles has changed (i.e., the *ankB* mutant has more packaging potential). The differ-

ence in quantities in membrane vesicles has been confirmed by thin sections (6).

(ii) Enhanced sensitivity to H$_2$O$_2$. Because we found that *ankB* is part of a small operon with *katB*, we postulated that its gene product may play a role in resistance to H$_2$O$_2$. To test this hypothesis, the wild type and *ankB*, *katB*, and *katB ankB* mutants were screened for H$_2$O$_2$ sensitivity. As shown in Fig. 7, an *ankB* mutant was only slightly more susceptible to H$_2$O$_2$ than wild-type organisms (bars 2). However, when the mutant was pretreated with a sublethal dose of H$_2$O$_2$, which activates the *katB*-*ankB* operon, sensitivity was increased dramatically (bars 2 versus bars 1 [shaded bars]). Bars 6 demonstrate that provision of a plasmid that allows for constitutive expression of *ankB* restored wild-type resistance regardless of H$_2$O$_2$ pretreatment. The *katB* (bars 3) and *katB ankB* (bars 4) mutants were equally susceptible to H$_2$O$_2$, and more so than the *ankB* mutant. Interestingly, provision of *ankB* alone to the *katB ankB* mutant dramatically helped these organisms resist H$_2$O$_2$ (bars 8 relative to bars 7).

(iii) Absence of AnkB decreases KatB activity. Because of the close proximity of *katB* and *ankB*, their organization in a small operon, and the enhanced H$_2$O$_2$ sensitivity of the *ankB* mutant, we postulated that AnkB could play a role in KatB function. To test this hypothesis, the catalase isozyme profiles of several mutant organisms were examined. Fig. 8 (left panel) shows that the KatB activities of the *ankB* mutant (lane 2) and a *katA ankB* (lane 5) mutant are significantly reduced relative to that of wild-type bacteria (lane 1). When transcription of *katB* was stimulated by the addition of paraquat, there was a robust increase in KatB activity in the wild type (right panel, lane 1) and especially in the *katA* mutant (right panel, lane 3). The catalase activity band produced in the *katA* mutant that migrated to the same R_f as KatA could be another, previ-
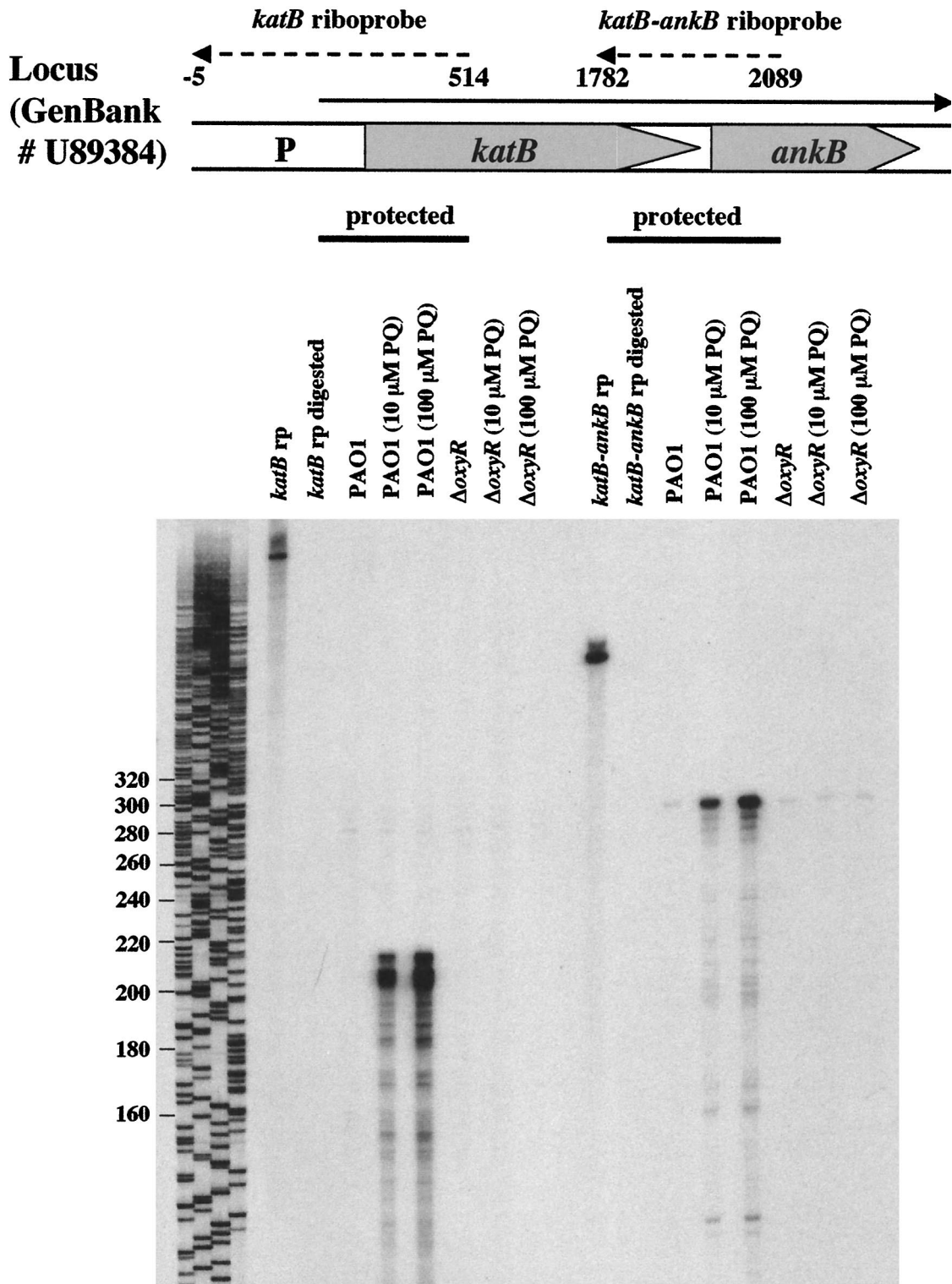
FIG. 5. RNase protection assays indicate that *katB* and *ankB* comprise an operon and are regulated by OxyR. Riboprobes specific for the *katB* promoter (*katB* rp) and for the *katB-ankB* overlapping region (*katB-ankB* rp) were used to detect the corresponding transcripts in *P. aeruginosa* PAO1 or *oxyR* mutant total RNA isolated during the exponential growth phase in aerobic M9 minimal medium. Paraquat (PQ) was added to final concentrations of 10 and 100 μM 1 h prior to harvest as indicated. Also shown are the digested probes in the absence of any *P. aeruginosa* RNA as a control. A DNA sequencing reaction was run in parallel and served as a size marker. Numbers on the left are base pairs.
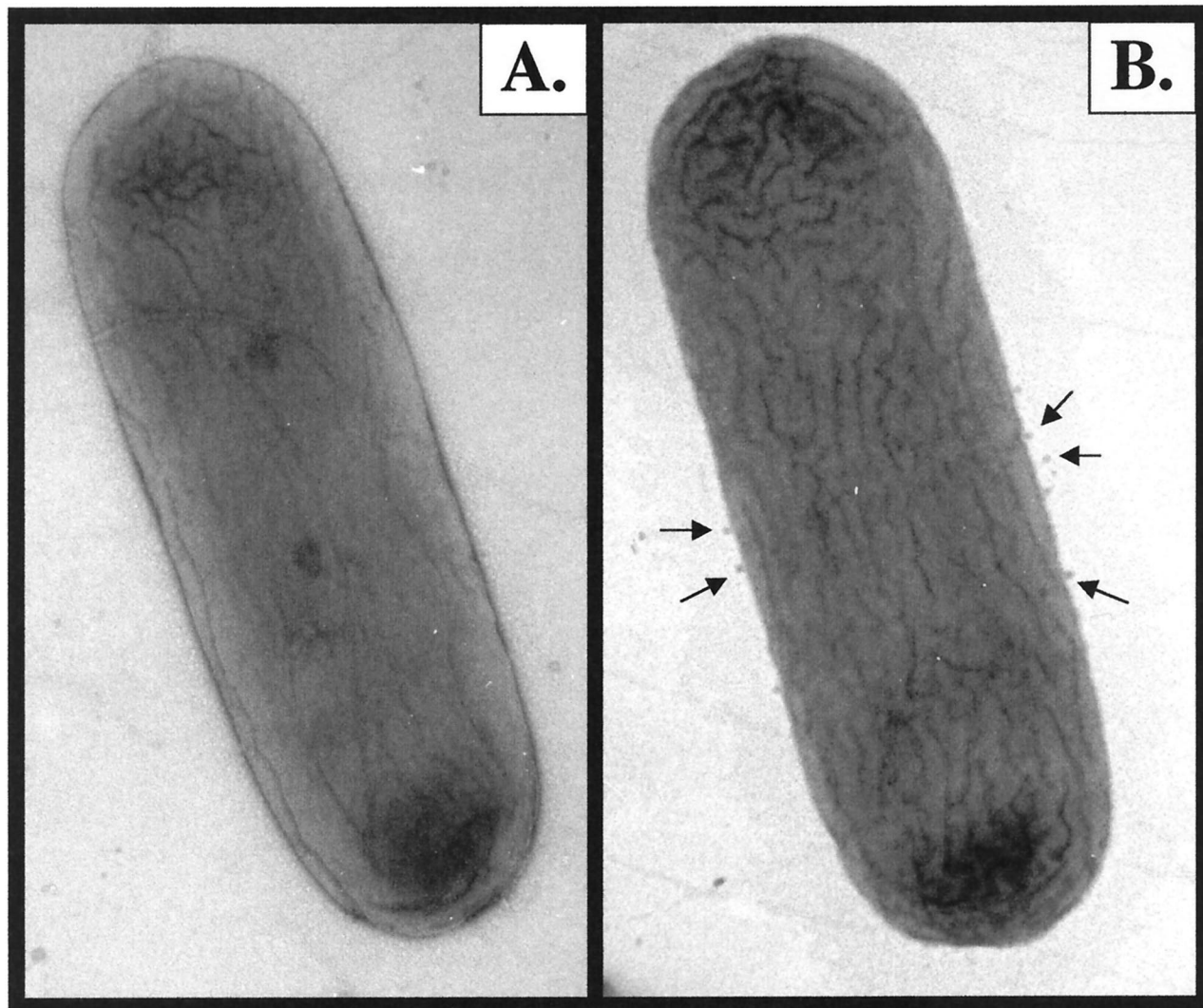
FIG. 6. Ultrastructural analysis of wild-type PAO (A) and PAO *ankB* mutant (B) bacteria. Bacteria were grown aerobically in L broth to mid-exponential growth phase and treated with 1 mM H_2O_2 for 1 h at 37°C to stimulate transcription of *katB-ankB*. Organisms were then prepared for TEM examination as described in Materials and Methods. The arrows in panel B point to the larger number of membrane vesicles being produced by the *ankB* mutant. The width of the cells is ~800 nm.

ously undiscovered catalase in *P. aeruginosa*, although analysis of the recently completed *P. aeruginosa* genome suggested otherwise (data not shown). We now know that this paraquat-inducible catalase band is one of the alkyl hydroperoxide reductases, AhpA, that possesses weak catalase activity (39). The KatB activities of the *ankB* mutant (Fig. 8, right panel, lane 2) and a *katA ankB* mutant (right panel, lane 5) were still reduced relative to that of wild-type bacteria (right panel, lane 1).

(iv) Quantitative effect of AnkB on KatB activity. To quantify the effect of AnkB on KatB activity, we examined catalase activity in *katA* and *katA ankB* mutants that had been treated with paraquat in stationary-phase culture, where the only catalase activity that can be detected and quantified spectrophotometrically is KatB. As shown in Fig. 9, the KatB activity of a paraquat-treated *katA* mutant is ~21.5 U/mg (bar 1). Provision of *ankB* in *trans* to the *katA* mutant had no effect on KatB activity (bar 2). Interestingly, KatB activity in a *katA ankB* mutant was reduced fourfold (bar 3) relative to that of the *katA*

mutant and was fully complemented by providing *ankB* in *trans* (bar 4). There was no observation of the AhpA activity band under these conditions.

DISCUSSION

The major catalase gene of *P. aeruginosa*, *katA*, encoding a constitutive 170-kDa heteromultimer, is positively regulated by iron (35) and maximally expressed in stationary phase, in part through a process of cell-to-cell communication known as quorum sensing (27). Thus, it is not surprising that KatA contributes significant protection against H_2O_2 in both planktonic and biofilm cultures (26, 27, 35).

In contrast to *katA*, which is minimally responsive to H_2O_2, we found in this study that the *katB-ankB* operon is transcribed dramatically in its presence and requires the global transactivator OxyR (25, 39). When we discovered *ankB* downstream of *katB*, we immediately classified its gene product as an ALP because it possessed the characteristic 33-amino-acid ank re-
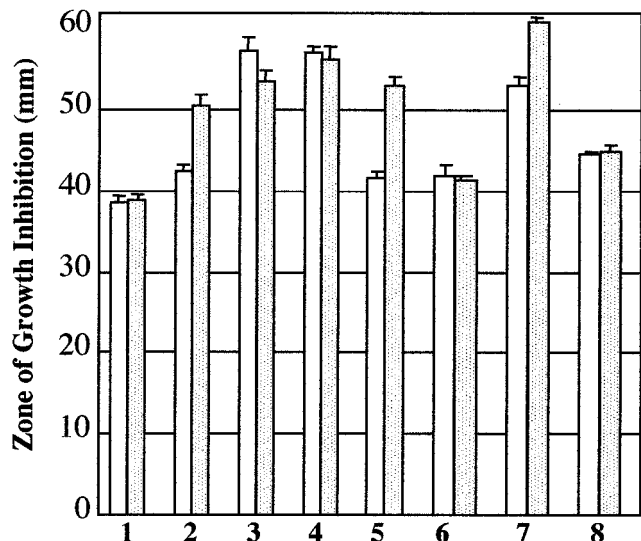
FIG. 9. Quantitative effect of AnkB on KatB activity. Bacteria were grown aerobically overnight in L-broth medium containing 0.35 mM paraquat at 37°C. Catalase activity and activity gel staining were monitored in cell extracts. Bars: 1, *katA* plus pUCP22; 2, *katA* plus p*ankB*; 3, *katA ankB* plus pUCP22; 4, *katA ankB* plus p*ankB*. Error bars indicate standard errors of the means. The inset photograph is KatB activity staining of cell extracts in a representative native polyacrylamide gel of each strain. It should be noted that no AhpA activity band (see Fig. 8) could be detected under these conditions.

FIG. 7. Effect of *ankB*, *katB*, and *katB ankB* on sensitivity to H_2O_2. All bacteria were grown aerobically overnight in M9F medium at 37°C. Fresh prewarmed medium (1 volume of culture in 10-volume flasks) was inoculated with 1/50 of the final culture volume and allowed to reach an OD_{600} of 0.6. Some bacteria were pretreated with a sublethal (1 mM) dose of H_2O_2 for 1 h (shaded bars) relative to control bacteria (open bars). The suspensions were diluted 100-fold in 7 ml of M9F 0.6% top agarose kept at 37°C and poured onto M9F plates. Filter paper disks (7 mm) impregnated with 8.8 M H_2O_2 were placed on the top agar surface. Zones of growth inhibition were measured after a 24-h aerobic incubation at 37°C. Bars: 1, PAO1; 2, *ankB*; 3, *katB*; 4, *katB ankB*; 5, *ankB* plus pUCP22; 6, *ankB* plus p*ankB*; 7, *katB ankB* plus pUCP22; 8, *katB ankB* plus p*ankB*. Error bars indicate standard errors of the means.

peat motifs and showed high similarity to ALPs in the related organisms *P. fluorescens* and *P. syringae* (32). Bacterial ALPs differ dramatically from their eukaryotic counterparts in that they contain only the ank repeats, which we believe to be involved in protein-protein interactions (5). Bacterial ALPs should, therefore, lack the structural role in the cell, similar to the function of prototypical erythrocyte spectrin-binding
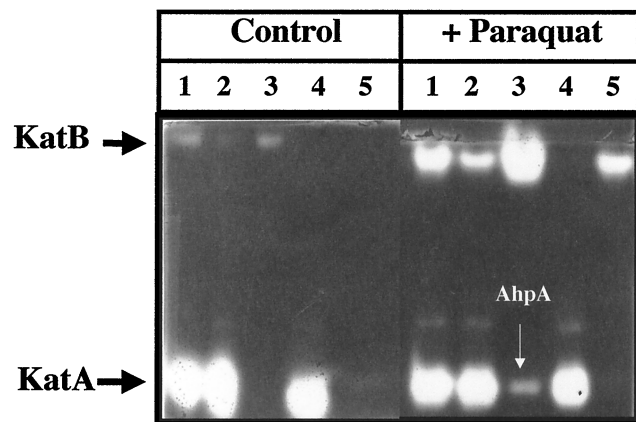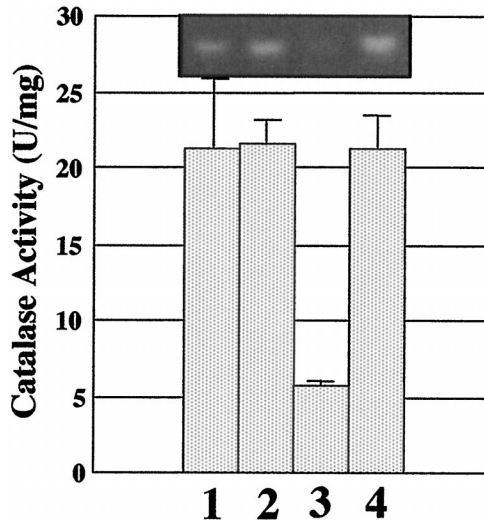

FIG. 8. Absence of AnkB causes a decrease in KatB activity. Bacteria were grown aerobically overnight in L-broth medium at 37°C. Fresh prewarmed medium (1 volume of culture in 10-volume flasks) was inoculated with 1/100 the final culture volume, and the organisms were grown to an OD_{600} of 0.6. Some bacteria (right panel) were then treated with a sublethal (0.35 mM) (11) dose of paraquat for 1 h, and the others (left panel) served as controls. Cell extracts were prepared, and 10 μg was subjected to nondenaturing polyacrylamide gel electrophoresis (5% polyacrylamide). The gels were then stained for catalase activity (58). Lanes: 1, PAO1; 2, *ankB*; 3, *katA*; 4, *katB*; 5, *katA ankB*.

ankyrin. Examination of transmission electron micrographs of the *ankB* mutant confirmed this assumption (Fig. 6). Due to the polycistronic nature of *katB-ankB* and the conservation of this operon in the pseudomonads and other proteobacteria such as *V. cholerae*, we postulated that AnkB might belong to a group of evolutionarily related proteins with a novel, unrecognized function(s), one of which could contribute toward protection against H_2O_2. Indeed, AnkB appears to play a role in the response of *P. aeruginosa* to H_2O_2, because an *ankB* mutant was more sensitive to it than wild-type organisms (Fig. 7). Furthermore, the enhanced H_2O_2 sensitivity of an isogenic *katB ankB* mutant did not change when only *katB* was provided in *trans* (39). Although unproven, the nearly fourfold reduction in KatB activity in the *ankB* mutant suggests that there could be a physical interaction between the two proteins. We found KatB activity in the cytoplasm, periplasm, and cytoplasmic membrane (data not shown). Because AnkB is a cytoplasmic membrane protein whose bitopic integration into the inner membrane ultimately causes its ank repeat domain to reside in the periplasm, we postulated that one function of AnkB may be to bind KatB near inner membrane targets that are sensitive to H_2O_2 (e.g., F_1F_o-ATPase [55]). H_2O_2 must first enter a protein channel leading to the heme catalytic site of the catalase molecule (47). Without entering this channel, the H_2O_2 is free to damage cellular components, especially sensitive respiratory chain components and DNA (16). Thus, AnkB may position or anchor KatB so that its H_2O_2 channel is in the optimal orientation for H_2O_2 entry. Alternatively, AnkB may serve to stabilize KatB, allowing it to persist longer and function better upon exposure of bacteria to H_2O_2.

An alternative hypothesis is that AnkB may reinforce the cytoplasmic membrane and prevent crippling of the proton motive force. Microscopic oxygen bubbles could be produced upon H_2O_2 degradation, thereby increasing cellular turgor pressure. Although unexplained, such cell swelling has been shown in *E. coli* (38) and in mitochondria treated with H_2O_2 or agents that generate it (30). Upon H_2O_2 degradation by cata-

lase, oxygen gas nuclei could be stabilized and even grow in the bacteria at hydrophobic sites. With the production of gas at a rate that saturates the cytoplasm, gas bubbles could readily appear, be stabilized by lipid and/or protein adsorption, and take up considerable volume inside a cell, thereby creating a turgor pressure (31). Thus, AnkB could serve to stabilize the inner membrane against swelling due to the mounting intracellular pressure built by H_2O_2 degradation. Both hypotheses are being tested experimentally.

ACKNOWLEDGMENTS

REFERENCES

1. **Altschul, S. F., W. Gish, W. Miller, E. W. Myers, and D. J. Lipman.** 1990. Basic local alignment search tool. J. Mol. Biol. **215:**403–410.
2. **Artavanis-Tsakonas, S., K. Matsuno, and M. E. Fortini.** 1995. Notch signaling. Science **268:**225–232.
3. **Barton, H., Z. Johnson, C. D. Cox, A. I. Vasil, and M. L. Vasil.** 1996. Ferric uptake regulator mutants of *Pseudomonas aeruginosa* with distinct alterations in the iron-dependent repression of exotoxin A and siderophores in aerobic and microaerobic environments. Mol. Microbiol. **4:**1001–1017.
4. **Beers, R. F., Jr., and I. W. Sizer.** 1952. A spectrophotometric method for measuring the breakdown of hydrogen peroxide by catalase. J. Biol. Chem. **195:**133–140.
5. **Bennett, V.** 1992. Ankyrins: adaptors between diverse plasma membrane proteins and the cytoplasm. J. Biol. Chem. **267:**8703–8706.
6. **Beveridge, T. J.** 1999. Structures of gram-negative cell walls and their derived membrane vesicles. J. Bacteriol. **181:**4725–4733.
7. **Bodine, D. M., C. S. Birkenmeier, and J. E. Barker.** 1984. Spectrin deficient inherited hemolytic anemias in the mouse: characterization by spectrin synthesis and mRNA activity in reticulocytes. Cell **37:**721–729.
8. **Bradford, M. M.** 1976. A rapid and sensitive method for the quantitation of microgram quantities of protein utilizing the principle of protein-dye binding. Anal. Biochem. **72:**248–254.
9. **Breeden, L., and K. Nasmyth.** 1987. Similarity between cell-cycle genes of budding yeast and fission yeast and the Notch gene of *Drosophila*. Nature **329:**651–654.
10. **Broome-Smith, J., and B. G. Spratt.** 1986. A vector for the construction of translational fusions to the TEM β-lactamase and analysis of protein export signals and membrane protein topology. Gene **49:**341–349.
11. **Brown, S. M., M. L. Howell, M. L. Vasil, A. J. Anderson, and D. J. Hassett.** 1995. Cloning and characterization of the *katB* gene of *Pseudomonas aeruginosa* encoding a hydrogen peroxide-inducible catalase: purification of KatB, cellular localization, and demonstration that it is essential for optimal resistance to hydrogen peroxide. J. Bacteriol. **177:**6536–6544.
12. **Burans, J. P., M. Lynn, and M. Solotorovsky.** 1983. Induction of active immunity with membrane fractions from *Haemophilus influenzae* type b. Infect. Immun. **41:**285–293.
13. **Calcutt, M. J., and F. J. Schmidt.** 1994. Gene organization in the bleomycin-resistance region of the producer organism *Streptomyces verticillus*. Gene **151:**17–21.
14. **Chan, T. A., C. A. Chu, K. A. Rauen, M. Kroiher, S. M. Tatarewicz, and R. E. Steele.** 1994. Identification of a gene encoding a novel protein-tyrosine kinase containing SH2 domains and ankyrin-like repeats. Oncogene **9:**1253–1259.
15. **Davis, J., and V. Bennett.** 1990. The anion exchanger and Na⁺K⁺ ATPase interacts with distinct sites on ankyrin: *in vitro* assays. J. Biol. Chem. **265:**17252–17256.
16. **Demple, B., and S. Linn.** 1982. 5,6-saturated lesions in DNA: production by ultraviolet light or hydrogen peroxide. Nucleic Acids Res. **10:**3781.
17. **Dolata, M. M., J. J. Van Beeumen, R. P. Ambler, T. E. Meyer, and M. A. Cusanovich.** 1993. Nucleotide sequence of the heme subunit of flavocytochrome *c* from the purple phototrophic bacterium, *Chromatium vinosum*: a 2.6-kilobase pair DNA fragment contains two multiheme cytochromes, a flavoprotein, and a homolog of human ankyrin. J. Biol. Chem. **268:**14426–14431.
18. **Elkins, J. G., D. J. Hassett, P. S. Stewart, H. P. Schweizer, and T. R. McDermott.** 1999. Protective role of catalase in *Pseudomonas aeruginosa* biofilm resistance to hydrogen peroxide. Appl. Environ. Microbiol. **65:**4594–4600.
19. **Fortini, M. E., and S. Artavanis-Tsakonas.** 1993. Notch: neurogenesis is only part of the picture. Cell **75:**1245–1247.

20. **Garen, A., and C. Levinthal.** 1960. A fine-structure genetic and chemical study of the enzyme alkaline phosphatase of *E. coli* I. Purification and characterization of alkaline phosphatase. Biochim. Biophys. Acta **38:**470.
21. **Givskov, M., L. Olsen, and S. Molin.** 1988. Cloning and expression in *Escherichia coli* of the gene for extracellular phospholipase A1 from *Serratia liquefaciens*. J. Bacteriol. **170:**5855–5862.
22. **Gorina, S., and N. P. Pavletich.** 1996. Structure of the p53 tumor suppressor bound to the ankyrin and SH3 domains of 53BP2. Science **274:**1001–1005.
23. **Greenfield, N., and G. D. Fasman.** 1969. Computed circular dichroism for the evaluation of protein conformation. Biochemistry **8:**4108–4116.
24. **Gutierrez, C., and J. C. Devedjian.** 1989. A plasmid facilitating in vitro construction of *phoA* gene fusions in *Escherichia coli*. Nucleic Acids Res. **17:**3999.
25. **Hassett, D. J., E. Alsabbagh, K. Parvatiyar, M. L. Howell, R. W. Wilmott, and U. A. Ochsner.** 2000. A protease-resistant catalase, KatA, released upon cell lysis during stationary phase is essential for aerobic survival of a *Pseudomonas aeruginosa oxyR* mutant at low cell densities. J. Bacteriol. **182:**4557–4563.
26. **Hassett, D. J., J. G. Elkins, J.-F. Ma, and T. R. McDermott.** 1999. *Pseudomonas aeruginosa* biofilm sensitivity to biocides: use of hydrogen peroxide as model antimicrobial agent for examining resistance mechanisms. Methods Enzymol. **310:**599–608.
27. **Hassett, D. J., J.-F. Ma, J. G. Elkins, T. R. McDermott, U. A. Ochsner, S. E. H. West, C.-T. Huang, J. Fredericks, S. Burnett, P. S. Stewart, G. McPheters, L. Passador, and B. H. Iglewski.** 1999. Quorum sensing in *Pseudomonas aeruginosa* controls expression of catalase and superoxide dismutase genes and mediates biofilm susceptibility to hydrogen peroxide. Mol. Microbiol. **34:**1082–1093.
28. **Holloway, B. W.** 1969. Genetics of *Pseudomonas*. Bacteriol. Rev. **33:**419–443.
29. **Holloway, B. W., V. Krishnapillai, and A. F. Morgan.** 1979. Chromosomal genetics of *Pseudomonas*. Microbiol. Rev. **43:**73–102.
30. **Kakkar, P., S. Mehrotra, and P. N. Viswanathan.** 1998. Influence of antioxidants on the peroxidative swelling of mitochondria *in vitro*. Cell Biol. Toxicol. **14:**313–321.
31. **Kim, D.** 1999. Elastic and viscous properties of fel-phase monolayers measured at the gas-bubble/water interface. Ph.D. thesis. Duke University, Durham, N.C.
32. **Klotz, M. G., and A. J. Anderson.** 1995. Sequence of a gene encoding periplasmic *Pseudomonas syringae* ankyrin. Gene **164:**187–188.
33. **Klotz, M. G., and S. W. Hutcheson.** 1992. Multiple periplasmic catalases in phytopathogenic strains of *Pseudomonas syringae*. Appl. Environ. Microbiol. **58:**2468–2473.
34. **Kraft, A. R., J. Prabhu, A. Ursinus, and J. V. Holtje.** 1999. Interference with murein turnover has no effect on growth but reduces beta-lactamase induction in *Escherichia coli*. J. Bacteriol. **181:**7192–7198.
35. **Ma, J.-F., U. A. Ochsner, M. G. Klotz, V. K. Nanayakkara, M. L. Howell, Z. Johnson, J. Posey, M. L. Vasil, J. J. Monaco, and D. J. Hassett.** 1999. Bacterioferritin A modulates catalase A (KatA) activity and resistance to hydrogen peroxide in *Pseudomonas aeruginosa*. J. Bacteriol. **181:**3730–3742.
36. **Michaely, P., and V. Bennett.** 1992. The ANK repeat: a ubiquitous motif involved in macromolecular recognition. Trends Cell Biol. **2:**127–130.
37. **Miller, J. H.** 1992. A short course in bacterial genetics, p. 72–74. Cold Spring Harbor Laboratory Press, Plainview, N.Y.
38. **Minakami, H., and I. Fridovich.** 1990. Effects of paraquat on cultures of *Escherichia coli*: turbidity versus enumeration. Free Rad. Biol. Med. **8:**387–391.
39. **Ochsner, U. A., M. L. Vasil, E. Alsabbagh, K. Parvatiyar, and D. J. Hassett.** 2000. Role of the *Pseudomonas aeruginosa oxyR-recG* operon in oxidative stress defense and DNA repair: OxyR-dependent regulation of *katB-ankB*, *ahpB*, and *ahpC-ahpF*. J. Bacteriol. **182:**4533–4544.
40. **Palek, J., and S. Lambert.** 1990. Genetics of the red cell membrane. Semin. Hematol. **27:**290–332.
41. **Peters, L. L., L. C. Turtzo, C. S. Birkenmeier, and J. E. Barker.** 1993. Distinct fetal Ank-1 and Ank-2 related proteins and mRNAs in normal and nb/nb mice. Blood **81:**2144–2149.
42. **Pugsley, A. P.** 1993. The complete secretory pathway in gram-negative bacteria. Microbiol. Rev. **57:**50–108.
43. **Schweizer, H. P.** 1991. Improved broad-host-range *lac*-based plasmid vectors for the isolation and characterization of protein fusions in *Pseudomonas aeruginosa*. Gene **103:**87–92.
44. **Schweizer, H. P.** 1994. A method for construction of bacterial hosts for *lac*-based cloning and expression vectors: α-complementation and regulated expression. BioTechniques **17:**452–456.
45. **Schweizer, H. P.** 1993. Small broad-host-range gentamicin resistance gene cassettes for site-specific insertion and deletion mutagenesis. BioTechniques **15:**831–833.
46. **Schweizer, H. P., and T. T. Hoang.** 1995. An improved system for gene replacement and *xylE* fusion analysis in *Pseudomonas aeruginosa*. Gene **158:**15–22.
47. **Sevinc, M. S., M. J. Mate, J. Switala, I. Fita, and P. C. Loewen.** 1999. Role of the lateral channel in catalase HPII of *Escherichia coli*. Protein Sci. **8:**490–498.

48. **Simon, R., U. Priefer, and A. Puehler.** 1983. A broad host range mobilization system for *in vivo* genetic engineering: transposon mutagenesis in gram negative bacteria. Bio/Technology **1:**784–791.

49. **Song, Y., and N. J. Sargentini.** 1996. *Escherichia coli* DNA repair gene *radA* and *sms* are the same gene. J. Bacteriol. **178:**5045–5048.

50. **Spence, A. M., A. Coulson, and J. Hodgkin.** 1990. The product of *fem-1*, a nematode sex-determining gene, contains a motif found in cell cycle control proteins and receptors for cell-cell interactions. Cell **60:**981–990.

51. **Srinivasan, Y., L. Elmer, J. Davis, V. Bennett, and K. Angelides.** 1988. Ankyrin and spectrin associate with voltage-dependent sodium channels in brain. Nature **333:**177–180.

52. **Srinivasan, Y., M. Lewallen, and K. J. Angelides.** 1992. Mapping the binding site of ankyrin for the voltage-dependent sodium channel from brain. J. Biol. Chem. **267:**7483–7489.

53. **Studier, F. W., and B. H. Moffatt.** 1986. Use of bacteriophage T7 RNA polymerase to direct selective high-level expression of cloned genes. J. Mol. Biol. **189:**113–130.

54. **Takemura, H., S. Horinouchi, and T. Beppu.** 1993. Suppression of an ethanol-sensitive mutation of *Acetobacter pasteurianus* by overexpression of the *his1* gene encoding histidinol phosphate aminotransferase. J. Ferment. Bioeng. **76:**224–228.

55. **Tamarit, J., E. Cabiscol, and J. Ros.** 1998. Identification of the major oxidatively damaged proteins in Escherichia coli cells exposed to oxidative stress. J. Biol. Chem. **273:**3027–3032.

56. **van de Goor, J., and R. B. Kelly.** 1996. Association of *Drosophila* cysteine string proteins with membranes. FEBS Lett. **19:**251–256.

57. **von Heijne, G.** 1992. Membrane protein structure prediction. Hydrophobicity analysis and positive-inside rule. J. Mol. Biol. **225:**487–494.

58. **Wayne, L. G., and G. A. Diaz.** 1986. A double staining method for differentiating between two classes of mycobacterial catalase in polyacrylamide gels. Anal. Biochem. **157:**89–92.